中国激光

组合光栅对半导体激光器的侧向模式调控作用

杜志方，范杰*，王海珠，邹永刚，马晓辉

长春理工大学高功率半导体激光国家重点实验室，吉林 长春 130022

摘要 设计并制作了一种新型含有组合光栅结构的分布式布拉格反射(CDBR)半导体激光器。通过引入组合光栅结构，对分布式布拉格反射(DBR)激光器的高阶侧向模式进行调控，提升了高阶侧向模式的损耗，最终优化了远场光斑图案。实验制得的器件腔长为 2 mm，脊波导宽度为 40 μm，高阶光栅周期为 7 μm，占空比为 0.6。当注入电流为 1.0 A 时，组合光栅起到明显作用，远场光斑图案从 DBR-激光二极管(LD)的多瓣优化到 CDBR-LD 的单瓣。CDBR-LD 在电流为 1.25 A 时的饱和输出功率约为 433 mW，斜率效率为 0.337 W•A^{-1}，注入电流为 0.95 A 时的光谱半峰全宽(FWHM)约为 0.61 nm。

关键词 激光器；半导体激光器；组合光栅；侧向模式；远场光斑；脊波导

中图分类号 TN365 **文献标志码** A **DOI**：10.3788/CJL230477

1 引 言

分布式布拉格反射(DBR)激光器由于体积小、易调制，被广泛应用于泵浦源、探测器、传感器、太阳能电池等领域中[1-8]。随着新型科技的出现与原有应用对激光光源需求的提升，人们对半导体激光器的侧向模式提出了更高要求。通过刻蚀较窄的脊波导结构可以限制高阶侧向模式，实现基侧模输出[9-10]，但是最大功率会因窄脊结构而受到限制。将窄脊波导与光放大器连接的激光器，在保证基侧模特性时，输出功率较高[11-12]，但是集成器件体型大，制作工艺复杂，且成品数量少。近年来中国科学院长春光学精密机械与物理研究所提出的宽脊波导器件刻蚀微结构的方式在实现器件侧向模式限制的同时可以保证良好的输出特性[13-14]，且 DBR 器件的研究主要集中于布拉格光栅的光谱研究，关于布拉格光栅对侧向模式分布的影响分析较少[15]。

本文设计并制作了一种含有组合光栅结构的宽脊波导 DBR 半导体激光器，研究了组合光栅结构对侧向模式的调控作用。器件的组合光栅区域既能调制器件的光谱特性，还可以起到限制高阶侧向模式损耗的作用，具有较高的输出功率。

2 器件设计制作及理论分析

2.1 器件设计制作

图 1(a)是含有组合光栅结构的分布式布拉格反射(CDBR)激光器的三维结构图，CDBR-激光二极管(LD)由脊波导和组合光栅区域构成，组合光栅由布拉格光栅区和混合光栅区组成。当激光器工作时，布拉格光栅区起到纵模反馈调制的作用，混合光栅区则对高阶侧向模式的损耗产生限制作用。器件的外延结构由单量子阱 $In_{0.26}GaAs/GaAsP_{0.16}$ 和对称波导层 $Al_{0.08}Ga_{0.92}As$ 组成，波导层介于 $Al_{0.23}Ga_{0.77}As$ 的限制层之间。器件参数图如图 1(b)、(c)所示，CDBR-LD 的器件腔长为 2 mm，脊波导宽度(W_{RW})为 40 μm。宽脊波导长度(L_{RW})为 1.3 mm，组合光栅区域长度(L_{CG})为 0.7 mm，由电感耦合等离子体(ICP)刻蚀一步刻蚀出。混合光栅区长度(L_{HG})为 0.35 mm，由渐变脊波导和两侧高阶布拉格光栅组成，另一同长度区域为高阶布拉格光栅区域(长度为 L_{BG})，渐变脊波导窄口宽度(W_G)为 15 μm，W_G 到 W_{RW} 呈线性变化，所有光栅周期为 7 μm，占空比为 0.6。对于制备得到的 CDBR-LD 和对比器件 DBR-LD，在未镀腔面膜的情况下，P 面向下且封装在热沉上，如图 1(d)所示，以供后续测试。

2.2 理论分析

根据半导体激光器谐振腔内的振荡过程，对组合光栅作用进行分步分析，普通脊波导区域的光进入混合光栅区域，定义此光为入射光。入射光经过混合光栅区域后再进入到高阶布拉格光栅区域发生反馈，此时反馈产生的光定义为反馈光。反馈光又经过混合光栅区域，最终回到脊波导中，完成一次振荡过程。在此基础之上探究组合光栅对各阶侧向模式的影响。

通过时域有限差分(FDTD)法中的 Mode 模块对器件混合光栅区域的侧向模式进行模拟计算，结果如图 2 所示，其中 TE_{00} 到 TE_{30} 代表基侧模到三阶

收稿日期：2023-02-01；**修回日期**：2023-04-01；**录用日期**：2023-04-28；**网络首发日期**：2023-05-08

基金项目：吉林省科技发展计划(20210201030GX)

通信作者：*fanjie@cust.edu.cn

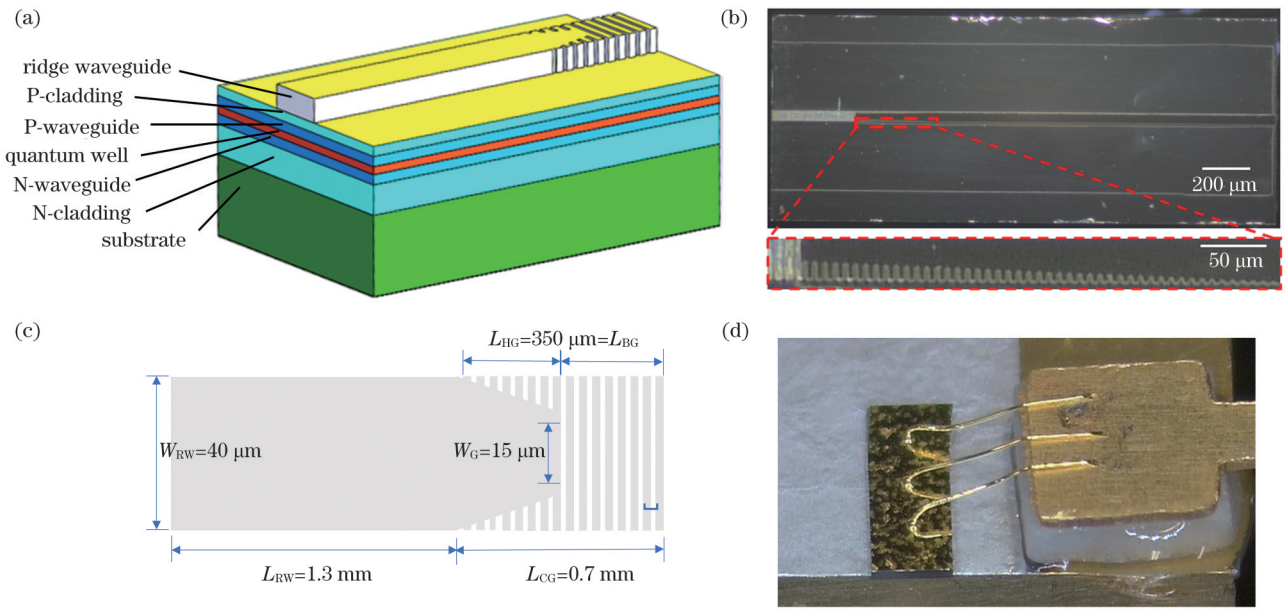

图 1　CDBR-LD 器件及结构参数图。(a)CDBR-LD 器件的三维结构图;(b)CDBR-LD 单管图片;(c)组合光栅结构及脊波导结构参数;(d)CDBR-LD 封装后的图片

Fig. 1　CDBR-LD device and structure parameters. (a) 3D structure diagram of CDBR-LD; (b) picture of CDBR-LD single tube; (c) structure parameters of combined grating and ridge waveguide; (d) photo of CDBR-LD after packaging

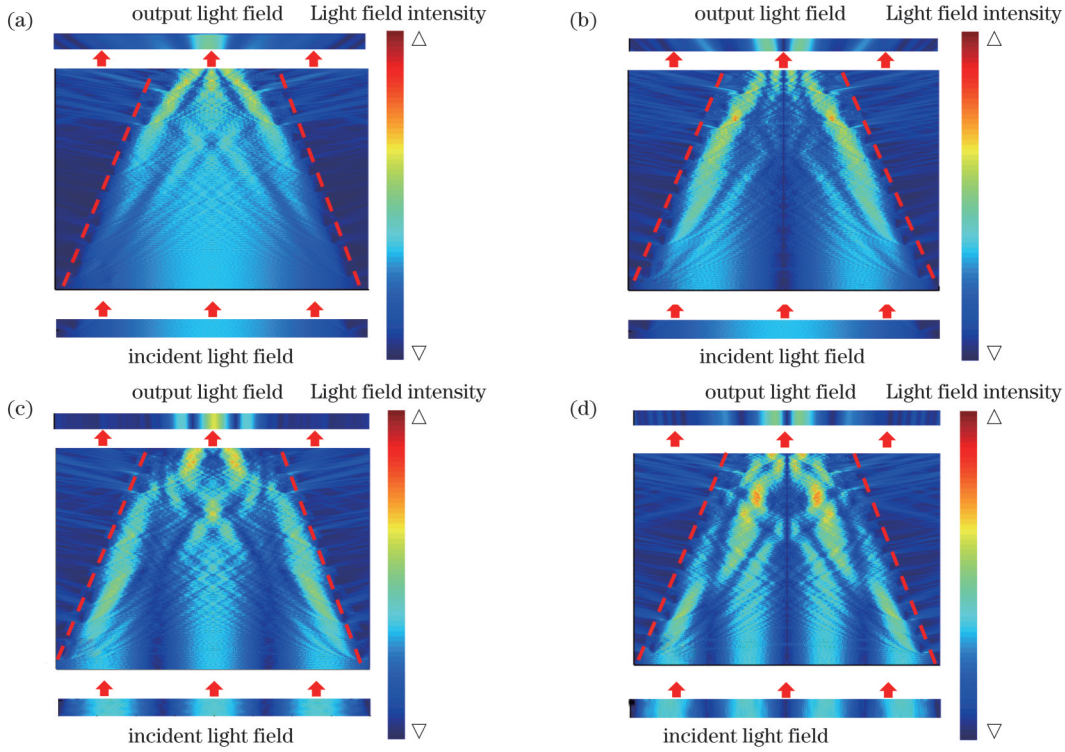

图 2　混合光栅区对入射光各阶侧向模式的影响。(a)TE_{00};(b)TE_{10};(c)TE_{20};(d)TE_{30}

Fig. 2　Influence of hybrid grating region on lateral mode of each order of incident light. (a) TE_{00}; (b) TE_{10}; (c) TE_{20}; (d) TE_{30}

侧向模式,虚线处是渐变脊波导和两侧光栅的交界线。在入射光情况下,基侧模(TE_{00})的光能量分布接近高斯光束能量分布,大部分能量集中在中间区域,所以在通过混合光栅区域时大多数能量得以保留,而只有少量能量在 W_G 较小的地方从边界处逸散,如图 2(a)所示。与基侧模不同,一阶侧向模式(TE_{10})的能量对称分布于两侧,因此在通过混合光栅区域时模式损耗更大。如图 2(b)所示,TE_{10} 大多数能量在边界处向外侧逸散,只有靠近中心的少量能量得以保留。同样对于更高阶的侧向模式,如二阶和三阶侧向模式 TE_{20} 和 TE_{30},由于模式阶数的升高,强度降低且分瓣多,能量更加分散,通过混合光

栅区域时在边界处会出现大量的能量逸散损耗，如图 2(c)、(d)所示，所以 L_{HG} 对入射光的高阶侧向模式起到调控作用。

图 2 中混合光栅区域出射的光，经高阶布拉格光栅区域反射产生了反馈光[16]。模拟了此反馈光经过混合光栅区域时各阶侧向模式受到的影响。基侧模 TE_{00} 的主要能量分布在中心位置处，所以大部分能量通过混合光栅区域后得以保留，少部分能量损耗，如图 3(a)所示。如图 3(b)～(d)所示，阶数更高的侧向模式，如一阶侧模 TE_{10} 到三阶侧模 TE_{30}，在混合光栅区域产生的损耗比基侧模更多。所以 L_{HG} 对反馈光的高阶侧向模式也能起到调控作用。

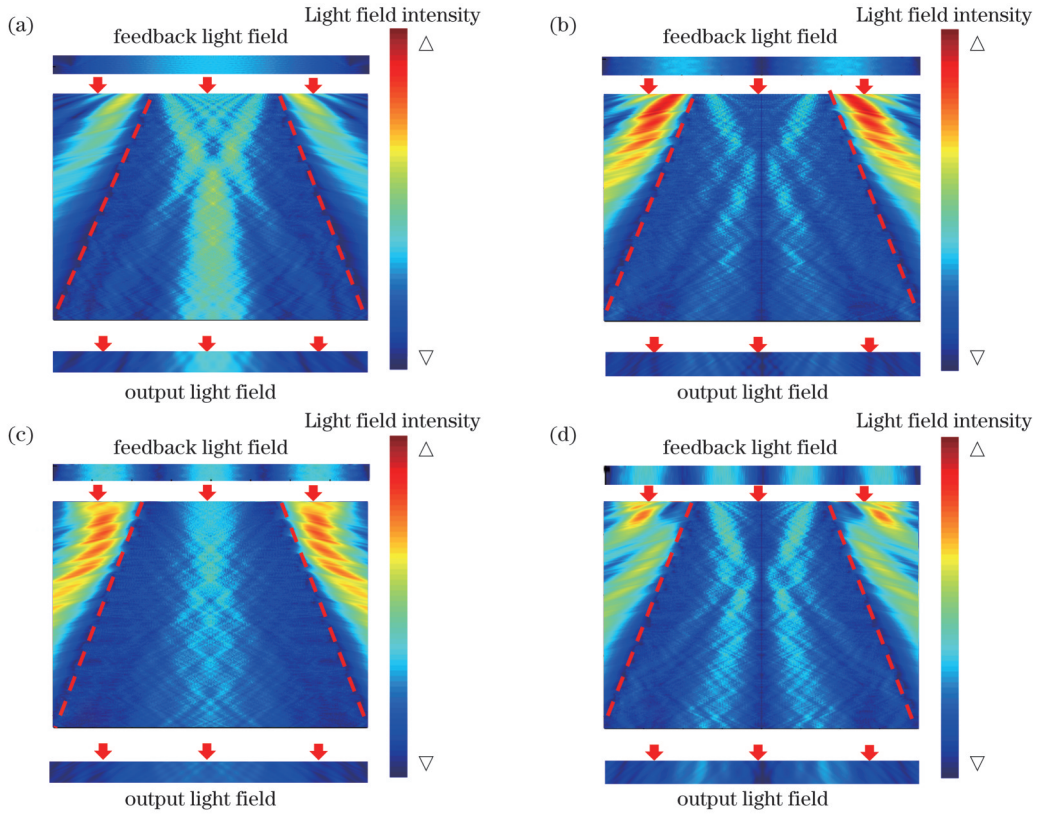

图 3　混合光栅区对反馈光各阶侧向模式的影响。(a)TE_{00}；(b)TE_{10}；(c)TE_{20}；(d)TE_{30}

Fig. 3　Influence of hybrid grating region on each order lateral mode of feedback light. (a) TE_{00}; (b) TE_{10}; (c) TE_{20}; (d) TE_{30}

入射光能量透过率的定义为：入射光进入混合光栅区域，出射的能量与入射能量的比值。如图 4 所示，当窄口宽度 W_G 不同时，对各阶侧向模式的透过率进行分析，右下角插图为基侧模 TE_{00} 与二阶侧模 TE_{20} 的透过率差(Δ)。入射光情况如图 4(a)所示，W_G 越小，逸散损耗区域越大，因此各阶侧向模式的能量透过率都比较低，当 W_G=5 μm 时，Δ 为 0.11，且所有侧向模式的能量损耗都较大。逐渐增大 W_G，模式

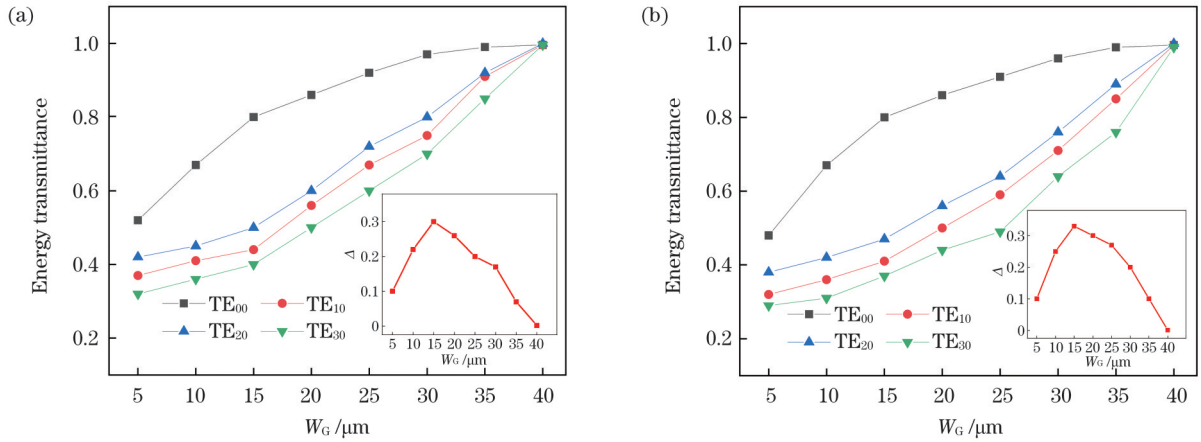

图 4　W_G 对各阶侧向模式能量透过率的影响(插图是 TE_{00} 与 TE_{20} 的能量透过率差)。(a)入射光；(b)反馈光

Fig. 4　Influence of W_G on energy transmittance of each order lateral mode with energy transmittance difference between TE_{00} and TE_{20} shown in inset. (a) Incident light; (b) feedback light

逸散损耗区域就开始减小，所有侧向模式的能量透过率增加，但由于各阶侧向模式的能量分布不同，在W_G增加到 15 μm 的过程中，基侧模 TE_{00}的能量透过率增长较快，而一阶侧模 TE_{10}到三阶侧模 TE_{30}的增长较为缓慢，当 W_G=15 μm 时，Δ=0.3。进一步增加W_G，基侧模 TE_{00}的能量透过率的增长速率放缓，而一阶侧模 TE_{10}到三阶侧模 TE_{30}的能量透过率的增长速率开始提升，此时混合光栅区的作用开始削弱，当 W_G=25 μm 时，Δ=0.2，差值缩小。直到 W_G增加到 40 μm，CDBR-LD 开始向 DBR-LD 过渡，混合光栅区变为普通脊波导区域，高阶侧向模式不再受限制，整体能量透过率基本相同，差值也逐渐消失，此时能量透过率为 1。

反馈光情况如图 4(b)所示，此时反馈光的能量透过率的定义为：入射光经过混合光栅区域，被高阶布拉格光栅反馈，产生的反馈光又进入混合光栅区域，此反馈光的出射能量与入射能量的比值。当 W_G=5 μm 时，所有侧向模式的损耗都较大，当 W_G=15 μm 时，Δ=0.33。当 W_G=25 μm 时，混合光栅区对高阶侧向模式的限制作用降低，Δ=0.27。当 W_G=40 μm 时，侧向模式的影响基本可以忽略不计。因此，混合光栅区域能够调控侧向模式。

3 测试结果与讨论

3.1 远场特性

CDBR-LD 与 DBR-LD 的远场特性由相机在室温 20 ℃条件下测得。图 5 所示是两器件在不同电流下的远场光斑及其能量图，横轴是远场光斑位置，纵轴为能量强度，其中光斑 x 方向为水平方向，y 方向是垂直方向，线图的横轴 Position 对应 x 方向。当注入电流从 0.7 A 增加到 1.0 A 时：对于 DBR-LD 器件，受谐振腔内高阶侧向模式的影响，模式竞争激烈，远场光斑明显分裂成多瓣，光斑图样受到严重影响，如图 5(a)、(c)所示；而对于 CDBR-LD，由于组合光栅对高阶侧向模式的调控作用，高能量高阶侧向模式被损耗，器件内部的模式竞争带来的影响降低，实现了远场光斑的单瓣输出，具有较好的远场光斑图案，如图 5(b)、(d)所示。由此可见，组合光栅确实能够起到调控侧向模式的作用。

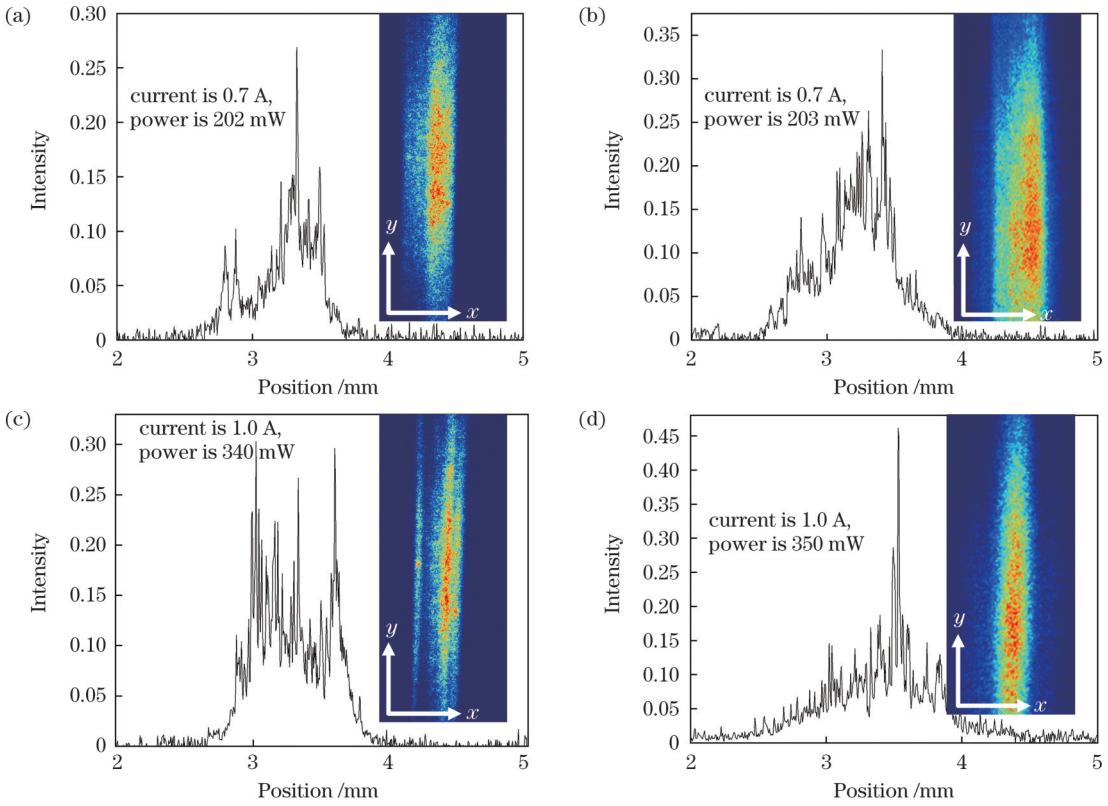

图 5 不同电流下 DBR-LD 和 CDBR-LD 的远场光斑和能量图。(a)注入电流 0.7 A，DBR-LD；(b)注入电流 0.7 A，CDBR-LD；(c)注入电流 1.0 A，DBR-LD；(d)注入电流 1.0 A，CDBR-LD

Fig. 5 Far-field spots and energy diagrams of DBR-LD and CDBR-LD at different currents. (a) DBR-LD, injection current of 0.7 A; (b) CDBR-LD, injection current of 0.7 A; (c) DBR-LD, injection current of 1.0 A; (d) CDBR-LD, injection current 1.0 A

3.2 光谱特性

在室温 20 ℃条件下，利用光谱仪在热电冷却(TEC)温控平台上对器件进行光谱测试，光谱仪精度约为 0.1 nm，测试结果如图 6 所示。DBR 激光器中布拉格光栅的存在，导致容易出现纵模的模式跳变现象，即输出波长从短波长向长波长方向移动且移动范围小[9,17-18]，再加上增加的注入电流导致的结温升高、波长红移，故 DBR-LD 和 CDBR-LD 的波长红移量比较

大。如图 6(a)所示，在注入电流从 0.35 A 逐渐增加到 0.95 A 的过程中，DBR-LD 的中心波长从 1031.87 nm 红移到 1036.1 nm，光谱半峰全宽（FWHM）从 1.17 nm 增加到 1.44 nm。图 6(b)所示为 CDBR-LD 的光谱变化，中心波长从 1031.25 nm 红移到 1037.15 nm，光谱半高宽从 0.50 nm 增加到 0.61 nm。对比发现，CDBR-LD 依旧能维持较好的光谱特性，且由于光栅区的绝对面积更大，光谱半峰全宽比 DBR-LD 器件更小。

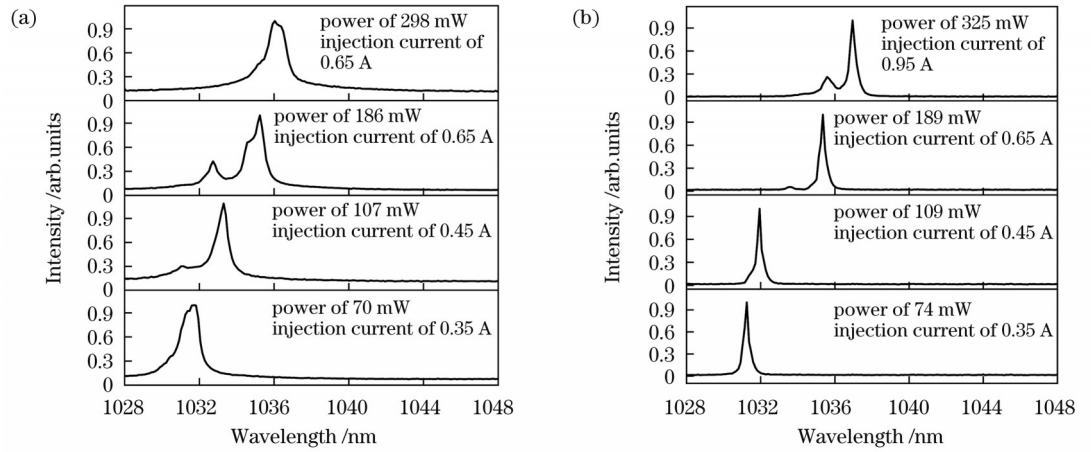

图 6　不同注入电流下 DBR-LD 和 CDBR-LD 的光谱。(a)DBR-LD；(b)CDBR-LD

Fig. 6　Spectra of DBR-LD and CDBR-LD under different injection currents. (a) DBR-LD; (b) CDBR-LD

3.3　功率特性

在室温 20 ℃条件下，利用功率计对 DBR-LD 和 CDBR-LD 的功率电流（*P-I*）曲线进行测试，结果如图 7 所示。两器件的阈值电流均为 0.1 A。DBR-LD 在注入电流为 1.2 A 时的饱和输出功率达到 406 mW，斜率效率为 0.333 mW·A^{-1}；对于 CDBR-LD，注入电流为 1.25 A 时的饱和输出功率达到 433 mW，斜率效率为 0.337 mW·A^{-1}。可见两器件的功率特性差别不大。由于组合光栅结构对高阶侧向模式的抑制作用，腔内模式竞争减少，CDBR-LD 的饱和功率出现略微提升[15,19-22]。

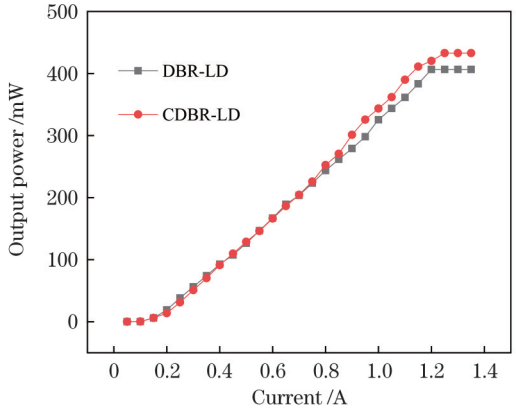

图 7　DBR-LD 和 CDBR-LD 的 *P-I* 曲线

Fig. 7　*P-I* curves of DBR-LD and CDBR-LD

4　结　　论

模拟研究并实验验证了组合光栅中的混合光栅区对各阶侧向模式的损耗作用，设计并制备了一种新型的含有组合布拉格光栅结构的分布式布拉格反射半导体激光器，器件中使用的高阶光栅对精度的要求比低阶光栅低且所需成本低，降低了工艺难度，制得的 CDBR-LD 在注入电流为 1.0 A 时实现了远场光斑的单瓣输出。CDBR-LD 在注入电流为 0.95 A 时的 FWHM 为 0.61 nm，注入电流为 1.25 A 时的饱和输出功率为 433 mW，斜率效率为 0.337 W·A^{-1}。

参　考　文　献

[1] 付星，刘廷昊，雷新星，等. 二极管泵浦重复频率纳秒高能固体激光器研究进展[J]. 中国激光，2021，48(15)：1501003.
Fu X，Liu T H，Lei X X，et al. High energy diode-pumped repetition-rated nanosecond solid-state laser[J]. Chinese Journal of Lasers，2021，48(15)：1501003.

[2] 薛家璧，赖寿强，刘欣，等. 基于 LED 泵浦的聚合物光波导吸收特性[J]. 中国激光，2021，48(20)：2006003.
Xue J B，Lai S Q，Liu X，et al. Realizing optical absorption properties of polymer waveguides using LED pump source[J]. Chinese Journal of Lasers，2021，48(20)：2006003.

[3] 李晋闽，刘志强，魏同波，等. 中国半导体照明发展综述[J]. 光学学报，2021，41(1)：0116002.
Li J M，Liu Z Q，Wei T B，et al. Development summary of semiconductor lighting in China[J]. Acta Optica Sinica，2021，41(1)：0116002.

[4] 李元栋，蒲涛，顾因，等. 基于直调光信号注入半导体激光器构建宽调谐可集成光电振荡器[J]. 光学学报，2022，42(13)：1323003.
Li Y D，Pu T，Gu Y，et al. Wide tuning integrated optoelectronic oscillator based on direct modulation optical signal injection semiconductor laser[J]. Acta Optica Sinica，2022，42(13)：1323003.

[5] Cui J S，Zhou Z P. High-performance Ge-on-Si photodetector with optimized DBR location[J]. Optics Letters，2017，42(24)：5141-5144.

[6] Lü C G，Liu Y，Wu C. Wide bandwidth dual-frequency ultrasound measurements based on fiber laser sensing technology[J]. Applied Optics，2016，55(19)：5057-5062.

[7] Sumpf B，Kabitzke J，Fricke J，et al. Dual-wavelength diode laser with electrically adjustable wavelength distance at 785 nm[J]. Optics Letters，2016，41(16)：3694-3697.

[8] Özen Y. The enhancement in cell performance of CdTe-based solar cell with Si/SiO_2 distributed Bragg reflectors[J]. Applied Physics

A, 2020, 126(8): 632.
[9] Chen H, Jia P, Chen C, et al. Narrow linewidth DBR laser based on high order Bragg grating defined by i-line lithography[J]. Optics Communications, 2019, 445: 296-300.
[10] Gwaro J O, Brenner C, Theurer L S, et al. Continuous wave THz system based on an electrically tunable monolithic dual wavelength Y-branch DBR diode laser[J]. Journal of Infrared, Millimeter, and Terahertz Waves, 2020, 41(5): 568-575.
[11] Zhang G, Ding Z H, Wang K K, et al. Demonstration of high output power DBR laser integrated with SOA for the FMCW LiDAR system[J]. Optics Express, 2022, 30(2): 2599-2609.
[12] Müller A, Fricke J, Bugge F, et al. DBR tapered diode laser with 12.7 W output power and nearly diffraction-limited, narrowband emission at 1030 nm[J]. Applied Physics B, 2016, 122(4): 87.
[13] Rong J M, Xing E B, Zhang Y, et al. Low lateral divergence 2 μm InGaSb/AlGaAsSb broad-area quantum well lasers[J]. Optics Express, 2016, 24(7): 7246-7254.
[14] Su J X, Tong C Z, Wang L J, et al. Beam waist shrinkage of high-power broad-area diode lasers by mode tailoring[J]. Optics Express, 2020, 28(9): 13131-13140.
[15] Wang Q Q, Xu L, Fan J E, et al. Lateral characteristics improvements of DBR laser diode with tapered Bragg grating[J]. Chinese Physics B, 2022, 31(9): 094204.
[16] Wang S. Principles of distributed feedback and distributed Bragg-reflector lasers[J]. IEEE Journal of Quantum Electronics, 1974, 10(4): 413-427.
[17] Ma P J, Jia Y F, Liu A J, et al. 30-Gbps directly modulated semiconductor lasers based on surface high-order gratings[J]. IEEE Photonics Technology Letters, 2021, 33(4): 197-200.
[18] Werner N, Blume G, Feise D, et al. Spectral mode hop characteristics of ridge waveguide lasers with distributed bragg-reflector[J]. IEEE Photonics Technology Letters, 2017, 29(24): 2183-2186.
[19] Crump P, Leisher P, Matson T, et al. Control of optical mode distribution through etched microstructures for improved broad area laser performance[J]. Applied Physics Letters, 2008, 92(13): 131113.
[20] Koester J P, Putz A, Wenzel H, et al. Mode competition in broad-ridge-waveguide lasers[J]. Semiconductor Science and Technology, 2021, 36(1): 015014.
[21] Tennant B A, Maywar D N. Single-mode distributed feedback lasing using photonic bandgaps to suppress degenerate modes[J]. Optics Letters, 2022, 47(13): 3367-3370.
[22] Jia P, Zhang J W, Chen Y Y, et al. Dual-wavelength emission from a high-order Bragg gratings integrated broad-area laser diode [J]. Optics & Laser Technology, 2022, 150: 107944.

Modulation Effect of Combined Grating on Lateral Modes of Semiconductor Laser

Du Zhifang, Fan Jie*, Wang Haizhu, Zou Yonggang, Ma Xiaohui

State Key Laboratory of High-Power Semiconductor Laser, Changchun University of Science and Technology, Changchun 130022, *Jilin, China*

Abstract

Objective Distributed Bragg reflector laser diodes (DBR-LDs) are widely used in pump sources, detectors, sensors, solar cells, and other applications because of their small size, long operating life, and high photoelectric conversion efficiency. With the development of modern technology and the demand for laser sources, higher requirements have been proposed for lateral modes of semiconductor lasers. The output of the fundamental lateral mode can be achieved by etching a narrow-ridge waveguide structure as this can limit the formation of higher-order lateral modes; however, it is difficult to further improve the maximum output power owing to the limitation of the narrow-ridge structure. Lasers, integrated by connecting a narrow-ridge waveguide to an optical amplifier, can obtain higher output power in the fundamental lateral mode. However, integrated devices are large, and the manufacturing process is complex. The method of etching microstructures on wide-ridge waveguide devices proposed in recent years ensures that the device overcomes lateral mode limitations and achieves excellent output performance. In addition, research on DBR devices has primarily focused on the spectral study of Bragg gratings. There has been less analysis of the influence of the Bragg grating on lateral mode distribution. In this study, a wide-ridge waveguide-based distributed Bragg reflector semiconductor laser with a combination grating structure (CDBR-LD) is designed and fabricated, and the influence of the combined grating structure on the modulation of lateral modes is investigated. The combination grating can modulate the spectral characteristics of the device and overcome higher-order lateral mode limitations.

Methods The internal action of a semiconductor laser resonator with a combined grating structure is analyzed and calculated using a finite-difference time-domain method. Owing to the complex internal actions of the device, the internal process is divided into two parts, which are analyzed separately: the incident light and feedback light . The combined grating consists of hybrid and Bragg grating areas. Herein, the incident light refers to the light from the direction of the ridge waveguide to the hybrid grating area (Fig. 2). The feedback light refers to the light from the Bragg grating area after the incident light is acted upon by the hybrid grating area (Fig. 3). According to the distribution law of lateral modes, the energy of the fundamental lateral modes is concentrated in the central region, whereas that of the higher-order lateral mode is dispersed. The loss mechanism of each order of the lateral modes in the incident light and feedback light in the hybrid grating area is analyzed. The value of the narrowest width of the mixed grating region is W_G; the effect of W_G on the energy transmittance of each order lateral mode is compared (Fig. 4). The ideal energy transmittance difference between the fundamental and the higher-order lateral modes is obtained with W_G of 15 μm. Therefore, the hybrid grating area in the combined grating structure can suppress the higher-order lateral modes of the device.

Results and Discussions According to the analysis of the far-field spots of the device (Fig. 5), spectra(Fig. 6), and the output power characteristics (Fig. 7), the far-field spot of the DBR-LD has significant spot-splitting as the injection current increases from 0.7 A to 1.0 A because of the strong mode competition caused by the higher-order lateral modes. The far-field spot-splitting effect of the CDBR-LD is significantly eliminated as the injection current increases from 0.7 A to 1.0 A because the loss of the higher-order lateral modes caused by the hybrid grating area reduces mode competition. This indicates that the combined grating structure can play a role in modulating the lateral modes of the DBR device. The DBR-LD has a red shift from 1031.87 nm to 1036.1 nm, and the full width at half maximum (FWHM) of the spectrum increases from 1.17 nm to 1.44 nm as the injection current varies from 0.35 A to 0.95 A. The CDBR-LD can maintain good spectral characteristics, which shows a red shift from 1031.25 nm to 1037.15 nm, and the FWHM of the spectrum increases from 0.5 nm to 0.61 nm. Moreover, the FWHM of the CDBR-LD spectrum is narrower than that of DBR-LD because CDBR-LD has a larger grating area. Finally, the DBR-LD exhibits a saturation output power of 406 mW at an injection current of 1.2 A with a slope efficiency of 0.333 mW/A. Additionally, the CDBR-LD exhibits a saturation output power of 433 mW at an injection current of 1.25 A with a slope efficiency of 0.337 mW/A.

Conclusions A DBR semiconductor laser with a combined grating structure is proposed in this study. By etching a hybrid grating area on the front side of the Bragg grating area, the loss of higher-order lateral modes increases and weakens the mode competition, eliminating the far-field spot-splitting phenomenon in wide-ridge waveguide DBR semiconductor lasers. Subsequently, a CDBR-LD is fabricated and tested. The experimental results show that the far-field spot splitting of CDBR-LD is significantly reduced as the injection current increases from 0.7 A to 1.0 A. The FWHM of the CDBR-LD spectrum is narrower than that of the DBR-LD as the injection current increases from 0.35 A to 0.95 A. A minimal difference is observed between the output powers of the DBR-LD and the CDBR-LD at an injection current of 1.2 A. In addition, the waveguide and grating structure of the CDBR-LD are etched in one step using the ultraviolet lithography, which has the advantages of being a simple process with a low cost. Based on these results, it is expected that a DBR semiconductor laser with good lateral-mode characteristics can be obtained by optimizing the structure.

Key words lasers; semiconductor lasers; combined grating; lateral mode; far-field spot; ridge waveguide